

AdaSample: Adaptive Sampling of Hard Positives for Descriptor Learning

Xin-Yu Zhang¹ Le Zhang² Zao-Yi Zheng¹ Yun Liu¹ Jia-Wang Bian³ Ming-Ming Cheng¹
¹TKLNDST, CS, Nankai University ²I2R, A*STAR ³The University of Adelaide

Abstract

Triplet loss has been widely employed in a wide range of computer vision tasks, including local descriptor learning. The effectiveness of the triplet loss heavily relies on the triplet selection, in which a common practice is to first sample intra-class patches (positives) from the dataset for batch construction and then mine in-batch negatives to form triplets. For high-informativeness triplet collection, researchers mostly focus on mining hard negatives in the second stage, while paying relatively less attention to constructing informative batches. To alleviate this issue, we propose AdaSample, an adaptive online batch sampler, in this paper. Specifically, hard positives are sampled based on their informativeness. In this way, we formulate a hardness-aware positive mining pipeline within a novel maximum loss minimization training protocol. The efficacy of the proposed method is evaluated on several standard benchmarks, where it demonstrates a significant and consistent performance gain on top of the existing strong baselines. The source codes will be released upon acceptance.

1. Introduction

Learning discriminative local descriptors from image patches is a fundamental ingredient of various computer vision tasks, including structure-from-motion [1], image retrieval [24], and panorama stitching [6]. Conventional approaches mostly utilize hand-crafted descriptors, such as SIFT [17], which have been successfully employed in a variety of applications. Recently, with the emergence of large-scale annotated datasets [3, 5], data-driven methods have started to demonstrate their effectiveness, and learning-based descriptors have gradually dominated this field. Specifically, convolutional neural network (CNN) based descriptors [10, 21, 30, 31, 34, 35] can achieve state-of-the-art performance on various tasks, including patch retrieval and 3D reconstruction.

Notably, *triplet loss* is adopted in many well-performing descriptor learning frameworks. Nevertheless, the quality of the learned descriptors heavily relies on the triplet selection, and mining suitable triplets from a large database

is a challenging task. Towards this challenge, Balntas *et al.* [4] propose an in-triplet hard negative mining strategy called anchor swapping. Tian *et al.* [30] progressively sample unbalanced training pairs in favor of negatives, and Mishchuk *et al.* [21] further simplify this idea to mine the hardest negatives within the mini-batch. Despite the significant progress on performance and generalization ability, however, two potential problems still exist in the current hardest-in-batch sampling solution: i) hard negatives are mined in the batch level, while randomly selected matching pairs can still be easily discriminated by the descriptor network; ii) it does not take the interaction between the training progress and the hardness of the training samples into consideration. To this end, we propose a novel triplet mining pipeline to adaptively construct high-informativeness batches in a principled manner.

Our proposed method is nominated as *AdaSample*, in which matching pairs are sampled from the dataset based on their *informativeness* to construct mini-batches. The methodology is developed on informativeness analysis, where *informativeness* is defined via the contributing gradients of the potential samples and can assist estimate their optimal sampling probabilities. Moreover, we propose a novel training protocol inspired by *maximum loss minimization* [26] to boost the generalization ability of the descriptor network. Under this training framework, we can adaptively adjust the overall hardness of the training examples fed to the network, based on the training progress. Comprehensive evaluation results and ablation studies on several standard benchmarks [3, 5] demonstrate the effectiveness of our proposed method.

In summary, our contributions are three-fold:

- We theoretically analyze the *informativeness* of potential training examples and formulate a principled sampling approach for descriptor learning.
- We propose a hardness-aware training protocol inspired by *maximum loss minimization*, in which the overall hardness of the generated triplets are adaptively adjusted to match the training progress.
- Comprehensive evaluation results on popular benchmarks demonstrate the efficacy of our proposed

AdaSample framework.

2. Related work

Local Descriptor Learning. Traditional descriptors [15, 17] mostly utilize hand-crafted features to extract low-level textures from image patches. The seminal work, *i.e.*, SIFT [17], computes the smoothed weighted histograms using the gradient field of the image patch. PCA-SIFT [15] further improves the descriptors by applying Principle Component Analysis (PCA) to the normalized image gradient. A comprehensive overview of the hand-crafted descriptors can be found in [20].

Recently, due to the rapid development of deep learning, CNN-based methods enable us to learn feature descriptors directly from the raw image patches. MatchNet [10] propose a two-stage Siamese architecture to extract feature embeddings and measure patch similarity, which significantly improves the performance and demonstrates the great potential of CNNs in descriptor learning. DeepDesc [27] trains the network with Euclidean distance and adopts a mining strategy to sample hard examples. DeepCompare [35] explores various architectures of the Siamese network and develops a two-stream network focusing on image centers.

With the advances of metric learning, triplet-based architectures have gradually replaced the pair-based ones. TFeat [4] adopts the triplet loss and mines in-triplet hard negatives with a strategy named anchor swapping. L2-Net [30] employs progressive sampling and requires that matching patches have minimal L2 distances within the mini-batch. HardNet [21] further develops the idea to mine the hardest-in-batch negatives with a simple triplet margin loss. DOAP [11] imposes a ranking-based loss directly optimized for the average precision. GeoDesc [18] further incorporates the geometric constraints from multi-view reconstructions and achieves significant improvement on 3D reconstruction task. SOSNet [31] proposes a second-order similarity regularization term and achieves more compact patch clusters in the feature space. A very recent work [36] relaxes the hard margin in the triplet margin loss with a dynamic soft margin to avoid manually tuning the margin by human heuristics.

From previous arts, we find that the triplet mining framework can generally be decoupled into two stages, *i.e.*, batch construction from the dataset and triplet generation within the mini-batch. Previous works [4, 21, 30] mostly focus on mining hard negatives in the second stage, while neglecting batch construction in the first place. Besides, their sampling approaches do not take the training progress into consideration when generating triplets. Therefore, we argue that their triplet mining solutions still cannot exploit the full potential of the entire dataset to produce triplets with suitable hardness. To alleviate this issue, we analyze the contributing gradients of the potential training examples and

sample informative matching pairs for batch construction. Then, we propose a hardness-aware training protocol inspired by *maximum loss minimization*, in which the overall hardness of the selected triplets is correlated with the training progress. Incorporating the hardest-in-batch negative mining solution, we formulate a powerful triplet mining framework, *AdaSample*, for descriptor learning, in which the quality of the learned descriptors can be significantly improved by a simple sampling strategy.

Hard Negative Mining. Hard negative mining has been widely used in deep metric learning, such as face verification [25], as it can progressively select hard negatives for triplet loss and Siamese networks to boost the performance and speed up the convergence. FaceNet [25] samples semi-hard triplets within the mini-batch to avoid overfitting the outliers. Wu *et al.* [33] select training examples based on their relative distances. Zheng *et al.* [38] augment the training data by adaptively synthesizing hardness-aware and label-preserving examples. However, our sampling solution differs from them in that we analyze the *informativeness* of the training data and ensure that the sampled data can provide gradients contributing most to the parameter update. Besides, our method can adaptively adjust the hardness of the selected training data as training progresses. In this way, well-classified samples are filtered out, and the network is always fed with informative triplets with suitable hardness. Comprehensive evaluation results demonstrate consistent performance improvement contributed by our proposed approach.

3. Methodology

3.1. Problem Overview

Given a dataset that consists of N classes¹ with each containing k matching patches, we decompose the triplet generation into two stages. Firstly, we select n matching pairs (positives) to form a mini-batch, where n is the batch size. This is done by our proposed *AdaSample*, as introduced in Sec. 3.2. Secondly, we mine the hardest-in-batch negatives for each matching pair and use the triplet loss to supervise the network training, as in Sec. 3.3. See Fig. 1 for an illustration of the two-stage sampling pipeline. Finally, the overall solution is summarized in Sec. 3.4.

3.2. AdaSample

Previous works [21, 30] sample positives randomly to construct mini-batches, yielding a majority of similar matching pairs which can be easily discriminated by the network. This practice may reduce the overall hardness of

¹ The term "class" stands for the image patches that come from the same 3D location. For our sampling purpose, patches from a single class are matching, while non-matching pairs come from different classes.

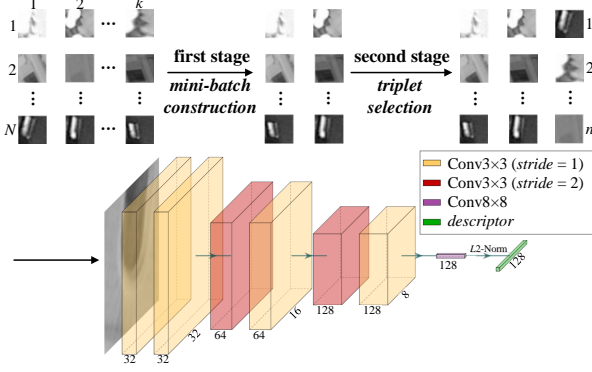


Figure 1. Illustration of the two-stage descriptor learning pipeline.

the triplets. Motivated by the hardest-in-batch mining strategy in [21], a straightforward solution is to select the most dissimilar matching pairs. However, potential issues arise, *i.e.*, the network may be trained with bias in favor of the most dissimilar matching pairs, while other cases are less-considered. We validate this solution, nominated as *Hardpos*, in experiments (Sec. 5.4).

A more principled solution is to sample positives based on their *informativeness*. Here, we assume that informative pairs are those contributing most to the optimization, namely, providing effective gradients for parameter updates. Therefore, we quantify the *informativeness* of the matching pairs by measuring their contributing gradients during training. Moreover, we employ *maximum loss minimization* [26] to improve the generalization ability of the learned model and show that the resulting gradient estimator is an *unbiased* estimator of the actual gradient. In the following, we introduce our derivation and elaborate on the theoretical justification in Sec. 4.

Informativeness Based Sampling. In the end-to-end deep learning literature, the training data contribute to optimization via gradients, so we measure the *informativeness* of training examples by analyzing their resulting gradients. Generally, we consider the generic deep learning framework. Let $(\mathbf{x}_i, \mathbf{y}_i)$ be the i^{th} data-label pair of the training set, $f(\mathbf{x}; \boldsymbol{\theta})$ be the model parameterized by $\boldsymbol{\theta}$, and $\mathcal{L}(\cdot, \cdot)$ be a differentiable loss function. The goal is to find the optimal model parameter $\boldsymbol{\theta}^*$ that minimizes the average loss, *i.e.*,

$$\boldsymbol{\theta}^* = \arg \min_{\boldsymbol{\theta}} \frac{1}{K} \sum_{i=1}^K \mathcal{L}(f(\mathbf{x}_i; \boldsymbol{\theta}), \mathbf{y}_i), \quad (1)$$

where K denotes the number of training examples. Then, we proceed with the following definition of *informativeness*.

Definition 1. The *informativeness* of a training example $(\mathbf{x}_i, \mathbf{y}_i)$ is quantified by its resulting gradient norm at it-

eration t , namely,

$$\text{info}(\mathbf{x}_i, \mathbf{y}_i) := \|\nabla_{\boldsymbol{\theta}_t} \mathcal{L}(f(\mathbf{x}_i; \boldsymbol{\theta}), \mathbf{y}_i)\|_2. \quad (2)$$

At iteration t , let $P_t = \{p_1^t, \dots, p_K^t\}$ be the sampling probabilities of each datum in the training set. More generally, we also re-weight each sample by w_1^t, \dots, w_K^t . Let random variable I_t denote the sampled index at iteration t , then $I_t \sim P_t$, namely, $\mathbb{P}(I_t = i) = p_i^t$. We record the re-weighted gradient induced by the training sample $(\mathbf{x}_i, \mathbf{y}_i)$ as

$$\mathbf{G}_i^t = w_i^t \nabla_{\boldsymbol{\theta}_t} \mathcal{L}(f(\mathbf{x}_i; \boldsymbol{\theta}), \mathbf{y}_i). \quad (3)$$

For simplicity, we omit the superscript t when no ambiguity is made. By setting $w_i = \frac{1}{K p_i}$, we can make the gradient estimator \mathbf{G}_i an unbiased estimator of the actual gradient, *i.e.*,

$$\mathbb{E}_{I_t \sim P_t} [\mathbf{G}_{I_t}] = \nabla_{\boldsymbol{\theta}_t} \frac{1}{K} \sum_{i=1}^K \mathcal{L}(f(\mathbf{x}_i; \boldsymbol{\theta}), \mathbf{y}_i). \quad (4)$$

Without loss of generality, we use stochastic gradient descent (SGD) to update model parameters:

$$\boldsymbol{\theta}_{t+1} = \boldsymbol{\theta}_t - \eta_t w_{I_t} \nabla_{\boldsymbol{\theta}_t} \mathcal{L}(f(\mathbf{x}_{I_t}; \boldsymbol{\theta}), \mathbf{y}_{I_t}) = \boldsymbol{\theta}_t - \eta_t \mathbf{G}_{I_t}, \quad (5)$$

where η_t is the learning rate at iteration t . As the goal is to find the optimal $\boldsymbol{\theta}^*$, we define the expected progress towards the optimum at each iteration as follows.

Definition 2. At iteration t , the *expected parameter rectification* R_t is defined as the expected reduction of the squared distance between the parameter $\boldsymbol{\theta}$ and the optimum $\boldsymbol{\theta}^*$ after iteration t ,

$$R_t := -\mathbb{E}_{I_t \sim P_t} [\|\boldsymbol{\theta}_{t+1} - \boldsymbol{\theta}^*\|_2^2 - \|\boldsymbol{\theta}_t - \boldsymbol{\theta}^*\|_2^2]. \quad (6)$$

Generally, tens of thousands of iterations are included in the training so that the empirical average parameter rectification will converge to the average of R_t asymptotically. Therefore, by maximizing R_t , we guarantee the most progressive step towards parameters optimum at each iteration in the expectation sense. Inspired by the *greedy algorithm* [8], we aim to maximize R_t at each iteration.

It can be shown that maximizing R_t is equivalent to minimizing $\text{tr}(\text{Var}[\mathbf{G}_{I_t}])$ (Thm. 1). Under this umbrella, we show that the optimal sampling probability is proportional to the per-sample gradient norm (a special case of Thm. 2). Therefore, the optimal sampling probability of each datum happens to be proportional to its *informativeness*. This property justifies our definition of *informativeness* as the resulting gradient norm of each training example.

However, as the neural network has multiple layers with a large number of parameters, it is computationally prohibitive to calculate the full gradient norm. Instead, we

prove that the matching distance in the feature space is a good approximation to the *informativeness*² in Sec. 4.2. Concretely, for each class consisting of k patches $\{\mathbf{X}_i : i = 1, \dots, k\}$, we first select a patch \mathbf{X}_{i_0} randomly, which serves as the anchor patch, and then sample a matching patch \mathbf{X}_i with probability

$$p_i \propto d(\mathbf{x}_i, \mathbf{x}_{i_0}), \text{ for } i \neq i_0, \quad (7)$$

where \mathbf{x}_i is the extracted descriptor of \mathbf{X}_i , and $d(\cdot, \cdot)$ measures the discrepancy of the extracted descriptors. See specific choices of d in Sec. 3.4.

Maximum Loss Minimization. Minimizing the average loss may be sub-optimal because the training tends to be overwhelmed by well-classified examples that provide noisy gradients [16]. On the contrary, well-classified examples can be adaptively filtered out by minimizing the maximum loss [26], which can further improve the generalization ability. However, directly minimizing the maximum loss may lead to insufficient usage of training data and sensitivity to outliers, so we approximate the gradient of maximum loss by $\nabla_{\theta_t} \frac{1}{K} \sum_{i=1}^K \mathcal{L}_i^\alpha$, in which α is sufficiently large. As \mathbf{G}_{I_t} is used to update parameters, consider its expectation

$$\mathbb{E}_{I_t \sim P_t} [\mathbf{G}_{I_t}] = \mathbb{E}_{I_t \sim P_t} [w_{I_t} \nabla_{\theta_t} \mathcal{L}_{I_t}] = \sum_{i=1}^K p_i w_i \nabla_{\theta_t} \mathcal{L}_i. \quad (8)$$

To guarantee \mathbf{G}_{I_t} is an unbiased estimator³ of $\nabla_{\theta_t} \frac{1}{K} \sum_{i=1}^K \mathcal{L}_i^\alpha$, it suffices to set

$$p_i w_i = \frac{\alpha}{K} \mathcal{L}_i^{\alpha-1}, \quad (9)$$

as in this case,

$$\mathbb{E}_{I_t \sim P_t} [\mathbf{G}_{I_t}] = \sum_{i=1}^K \frac{\alpha}{K} \mathcal{L}_i^{\alpha-1} \nabla_{\theta_t} \mathcal{L}_i = \sum_{i=1}^K \frac{1}{K} \nabla_{\theta_t} \mathcal{L}_i^\alpha. \quad (10)$$

Following the previous reasoning, we need to minimize $\text{tr}(\text{Var}[\mathbf{G}_{I_t}])$ under the constraints specified by Eqn. 9 in order to step most progressively at each iteration. In Thm. 2, we show that the optimal sampling probability and re-weighting scalar should be given by

$$p_i \propto \mathcal{L}_i^{\alpha-1} \|\nabla_{\theta_t} \mathcal{L}_i\|_2 \text{ and } w_i \propto \|\nabla_{\theta_t} \mathcal{L}_i\|_2^{-1}. \quad (11)$$

²The approximation is up to a constant factor, which is insignificant as it will be offset by the learning rate. The same reasoning applies to the approximation of gradients in **Maximum Loss Minimization** paragraph.

³We impose the unbiasedness constraints due to its theoretical convergence guarantees. For example, the non-asymptotic error bound induced by unbiased gradient estimates is referred to [22]. For re-weighted SGD, as in our case, improved convergence rate can be found in [23].

As previously claimed, we approximate the gradient norm via the matching distance in the feature space. Besides, in our case, the hinge triplet loss (Eqn. 14) is positively (or even linearly) correlated with the matching distance squared. Therefore, we use the matching distance squared as an approximation of the hinge triplet loss. Thus, the sampling probability and re-weighting scalar are given by

$$p_i \propto d(\mathbf{x}_i, \mathbf{x}_{i_0})^{2\alpha-1} \text{ and } w_i \propto d(\mathbf{x}_i, \mathbf{x}_{i_0})^{-1}, \text{ for } i \neq i_0. \quad (12)$$

Moreover, for better approximation, it is preferable to adjust α adaptively, namely, to increase α with training. Intuitively, when easy matching pairs have been correctly classified, we focus more on hard ones. A good indicator of the training progress is the *average loss*. As a result, instead of pre-defining a sufficiently large α , we set $2\alpha - 1 = \lambda / \mathcal{L}_{avg}$, where λ is a tunable hyperparameter, and \mathcal{L}_{avg} is the moving average of history loss. Formally, we formulate our sampling probability and re-weighting scalar as

$$p_i \propto d(\mathbf{x}_i, \mathbf{x}_{i_0})^{\frac{\lambda}{\mathcal{L}_{avg}}} \text{ and } w_i \propto d(\mathbf{x}_i, \mathbf{x}_{i_0})^{-1}, \text{ for } i \neq i_0. \quad (13)$$

The exponent increases adaptively as training progresses so that hardness-aware training examples can be generated and fed to the network. Our sampling approach is thus named as *AdaSample*.

3.3. Triplet generation by hardest-in-batch

AdaSample focuses on the batch construction stage, and for a complete triplet mining framework, we need to mine negatives from the mini-batch as well. Here, we adopt the hardest-in-batch strategy in [21]. Formally, given a mini-batch of n matching pairs $\{(\widetilde{\mathbf{X}}_i, \widetilde{\mathbf{X}}_i^+) : i = 1, \dots, n\}$, let $(\widetilde{\mathbf{x}}_i, \widetilde{\mathbf{x}}_i^+)$ be the descriptors extracted from $(\widetilde{\mathbf{X}}_i, \widetilde{\mathbf{X}}_i^+)$ ⁴. For each matching pair $(\widetilde{\mathbf{X}}_i, \widetilde{\mathbf{X}}_i^+)$, we select the non-matching patch which lies closest to one of the matching patches in the feature space. Then, the Hinge Triplet (HT) loss is defined as follows:

$$\begin{aligned} \mathcal{L}_i &= \max \{t + (d_i^{pos})^2 - (d_i^{neg})^2, 0\}, \\ d_i^{pos} &= d(\widetilde{\mathbf{x}}_i, \widetilde{\mathbf{x}}_i^+), \\ d_i^{neg} &= \min_{j \neq i} \{ \min \{d(\widetilde{\mathbf{x}}_i, \widetilde{\mathbf{x}}_j), d(\widetilde{\mathbf{x}}_i^+, \widetilde{\mathbf{x}}_j^+)\} \}, \end{aligned} \quad (14)$$

where t denotes the margin. Incorporating the re-weighting scalar, we update the model parameter via the gradient estimator $\sum_{i=1}^n w_i \nabla_{\theta} \mathcal{L}_i$.

⁴For clarity, $(\widetilde{\mathbf{X}}_\diamond, \widetilde{\mathbf{X}}_\diamond^+)$ denotes the selected matching pairs, with different pairs belonging to different classes. \mathbf{X}_\diamond denotes a generic patch in a specific class, where \diamond denotes the placeholder for the index.

Algorithm 1 Pipeline of *AdaSample* framework.

Require:

- Dataset of N classes with each containing k matching patches;
 - Moving average of history loss \mathcal{L}_{avg} ;
 - Hyperparameter λ ;
 - 1: Randomly select n distinct classes from the dataset without replacement;
 - 2: Extract descriptors of the patches belonging to the selected classes;
 - 3: **for** each selected class with k patches $\{\mathbf{X}_i : i = 1, \dots, k\}$ **do**
 - 4: Sample an anchor patch \mathbf{X}_{i_0} randomly;
 - 5: Sample a matching patch \mathbf{X}_i from the remaining patches with probabilities specified by Eqn. 13;
 - 6: **end for**
 - 7: With sampled positive pairs and their descriptors $\{(\tilde{\mathbf{x}}_i, \tilde{\mathbf{x}}_i^+)\}_{i=1}^n$, compute Angular Triplet Hinge loss by Eqn. 15;
 - 8: Backpropagate and update model parameters via $\sum_{i=1}^n w_i \nabla_{\theta} \mathcal{L}_i$;
-

3.4. Distance Metric

Euclidean distance is widely used in previous works [21, 27, 30, 31]. However, as the descriptors lie on the unit hypersphere in 128-dimensional space (Sec. 5.1), it is more natural to adopt the geodesic distance of the embedded manifold. Therefore, we adopt the angular distance [7] as follows:

$$d(\tilde{\mathbf{x}}_1, \tilde{\mathbf{x}}_2) = \arccos(\tilde{\mathbf{x}}_1 \cdot \tilde{\mathbf{x}}_2), \quad (15)$$

where \cdot denotes the inner product operator. We nominate our loss function as Angular Hinge Triplet (AHT) loss, which is demonstrated to result in consistent performance improvement (Sec. 5.4).

Alg. 1 summarizes the overall triplet generation framework. For each training iteration, we first randomly pick n distinct classes from the dataset and extract descriptors for patches belonging to these classes (Step 1, 2). Then, we randomly choose a patch as the anchor from each of the selected classes (Step 4) and adopt our proposed *AdaSample* to select an informative matching patch (Step 5). With the generated mini-batch, we mine hard negatives following [21] and compute Angular Hinge Triplet (AHT) loss (Step 7).

4. Theoretical Analysis

In this section, we complete the theoretical analysis of *informativeness* in Sec. 4.1, and prove that the matching distance can serve as a good approximation of *informativeness* in Sec. 4.2.

4.1. Informativeness Formulation

Following notations in Sec. 3.2, we reformulate R_t (Eqn. 6), and give an equivalent condition for maximizing R_t . The same conclusion can be found in [14].

Theorem 1. Let R_t , θ^* , and \mathbf{G}_i be defined as in Eqn. 6, 1

and 3, respectively. Then, we have

$$R_t = 2\eta_t(\theta_t - \theta^*)^T \mathbb{E}_{I_t \sim P_t} [\mathbf{G}_{I_t}] - \eta_t^2 \mathbb{E}_{I_t \sim P_t} [\mathbf{G}_{I_t}]^T \mathbb{E}_{I_t \sim P_t} [\mathbf{G}_{I_t}] - \eta_t^2 \text{tr}(\text{Var} [\mathbf{G}_{I_t}]). \quad (16)$$

Due to unbiasedness (Eqn. 4), the first two terms in Eqn. 16 is fixed, so maximizing R_t is equivalent to minimizing $\text{tr}(\text{Var} [\mathbf{G}_{I_t}])$. Thm. 2 specifies the optimal probabilities to minimize the aforementioned trace under a more general assumption.

Theorem 2. Let \mathbf{G}_i be defined in Eqn. 3 and suppose the sampled index I_t obeys distribution P_t . Then, given the constraints $p_i w_i = \frac{\alpha}{K} \mathcal{L}_i^{\alpha-1}$, $\text{tr}(\text{Var} [\mathbf{G}_{I_t}])$ is minimized by the following optimal sampling probabilities:

$$p_i = \frac{1}{Z} \mathcal{L}_i^{\alpha-1} \|\nabla_{\theta_t} \mathcal{L}_i\|_2, \text{ where } Z = \sum_{j=1}^K \mathcal{L}_j^{\alpha-1} \|\nabla_{\theta_t} \mathcal{L}_j\|_2. \quad (17)$$

Proof. As \mathbf{G}_{I_t} is an unbiased estimator of the actual gradient (Eqn. 4), $\mathbb{E}_{I_t \sim P_t} [\mathbf{G}_{I_t}]$ is fixed in our case, denoted by μ for short. By the linearity of trace and $\text{tr}(\mu\mu^T) = \|\mu\|_2^2$, we have

$$\begin{aligned} \text{tr}(\text{Var} [\mathbf{G}_{I_t}]) &= \text{tr}(\mathbb{E}_{I_t \sim P_t} [(\mathbf{G}_{I_t} - \mu)(\mathbf{G}_{I_t} - \mu)^T]) \\ &= \text{tr}(\mathbb{E}_{I_t \sim P_t} [\mathbf{G}_{I_t} \mathbf{G}_{I_t}^T - \mu\mu^T]) \\ &= \mathbb{E}_{I_t \sim P_t} [\text{tr}(\mathbf{G}_{I_t} \mathbf{G}_{I_t}^T)] - \text{tr}(\mu\mu^T) \\ &= \mathbb{E}_{I_t \sim P_t} [\|\mathbf{G}_{I_t}\|_2^2] - \|\mu\|_2^2 \\ &= \sum_{i=1}^K p_i w_i^2 \|\nabla_{\theta_t} \mathcal{L}_i\|_2^2 - \|\mu\|_2^2 \\ &= \frac{\alpha^2}{K^2} \sum_{i=1}^K \frac{\mathcal{L}_i^{2\alpha-2} \|\nabla_{\theta_t} \mathcal{L}_i\|_2^2}{p_i} - \|\mu\|_2^2. \end{aligned} \quad (18)$$

Mathematically, given the constraints $\sum_{i=1}^K p_i = 1$, the aforementioned harmonic mean of $\{p_1, \dots, p_K\}$ reaches its minimum when the probabilities satisfy

$$p_i \propto \mathcal{L}_i^{\alpha-1} \|\nabla_{\theta_i} \mathcal{L}_i\|_2. \quad (19)$$

Dividing by a normalization factor, we get the expression in Eqn. 17. \square

Note that in the special case of $\alpha = 1$, the constraints degrade into $p_i w_i = \frac{1}{K}$, and the optimal sampling probabilities become $p_i \propto \|\nabla_{\theta_i} \mathcal{L}_i\|_2$.

4.2. Approximation of Informativeness

As mentioned in Sec. 3.2, the matching distance can serve as a good approximation of *informativeness*. We justify this here. For simplicity, we introduce some notations for a L -layer multi-layer perceptron (MLP). Let $\theta^{(l)} \in \mathbb{R}^{M_l \times M_{l-1}}$ be the weight matrix for layer l and $g^{(l)}$ be a Lipschitz continuous activation function. Then the multi-layer perceptron can be formulated as follows:

$$\begin{aligned} \mathbf{x}^{(0)} &= \mathbf{x}, \\ \mathbf{h}^{(l)} &= \theta^{(l)} \mathbf{x}^{(l-1)}, \text{ for } l = 1, \dots, L, \\ \mathbf{x}^{(l)} &= g^{(l)}(\mathbf{h}^{(l)}), \text{ for } l = 1, \dots, L, \\ f(\mathbf{x}; \theta) &= \mathbf{x}^{(L)}, \\ \theta &= \{\theta^{(1)}, \dots, \theta^{(L)}\}. \end{aligned} \quad (20)$$

Note that although our notations describe only MLPs without bias, our analysis holds for any affine transformation followed by a Lipschitz continuous non-linearity. Therefore, our reasoning can naturally extend to CNNs. With

$$\begin{aligned} \Gamma_l(\mathbf{h}^{(l)}) &= \text{diag} \left\{ g'^{(l)}(h_1^{(l)}), \dots, g'^{(l)}(h_{M_l}^{(l)}) \right\}, \\ \Pi^{(l)} &= \Gamma_l(\mathbf{h}^{(l)}) \theta_{l+1}^T \cdots \Gamma_{L-1}(\mathbf{h}^{(L-1)}) \theta_L^T \Gamma_L(\mathbf{h}^{(L)}), \end{aligned} \quad (21)$$

we have

$$\begin{aligned} \|\nabla_{\theta_l} \mathcal{L}(f(\mathbf{x}; \theta), \mathbf{y})\|_2 &= \left\| \left(\Pi^{(l)} \nabla_{\mathbf{x}^{(L)}} \mathcal{L} \right) \left(\mathbf{x}^{(l-1)} \right)^T \right\|_2 \\ &\leq \|\Pi^{(l)}\|_2 \|\mathbf{x}^{(l-1)}\|_2 \|\nabla_{\mathbf{x}^{(L)}} \mathcal{L}\|_2. \end{aligned} \quad (22)$$

Various data preprocessing, weight initialization [9, 12], and activation normalization [2, 13, 32] techniques uniformize the activations of each layer across samples. Therefore, the variation of gradient norms is mostly captured by the gradient of the loss function *w.r.t.* the output of neural networks,

$$\text{info}(\mathbf{x}, \mathbf{y}) = \|\nabla_{\theta} \mathcal{L}(f(\mathbf{x}; \theta), \mathbf{y})\|_2 \approx M \|\nabla_{\mathbf{x}^{(L)}} \mathcal{L}\|_2, \quad (23)$$

where M is a constant, and $M \|\nabla_{\mathbf{x}^{(L)}} \mathcal{L}\|_2$ serves as a precise approximation of the full gradient norm. For simplicity, we consider hinge triplet loss (Eqn. 14) here. Then, the gradient norm *w.r.t.* the descriptor of the matching patch is just twice the matching distance⁵,

$$\|\nabla_{\mathbf{x}^{(L)}} \mathcal{L}\|_2 = 2d^{\text{pos}}. \quad (24)$$

As a result, we reach the conclusion that the matching distance is a good approximation to the *informativeness*. Also, we empirically verify this in Sec. 5.4.

5. Experiments

5.1. Implementation Details

We adopt the architecture of L2-Net [30] to embed local descriptors into the unit hypersphere in 128-dimensional space. Following prior works [21, 30], all patches are resized to 32×32 and normalized to zero per-patch mean and unit per-patch variance. We train our model from scratch in PyTorch library [29] using SGD optimizer with initial learning rate $\eta = 10$, momentum 0.5, and weight decay 0.0001. Batch size is 1024, margin $t = 1$, and $\lambda = 10$ unless otherwise specified. We generate 1,000,000 matching pairs for each epoch, and the total number of epochs is 90. The learning rate is divided by 10 at the end of 30, 60, 80 epochs.

We compare our method with both handcrafted and deep methods⁶, including SIFT [17], DeepDesc [28], TFeat [4], L2-Net [30], HardNet [21], HardNet with global orthogonal regularization (GOR) [37], DOAP [11], and GeoDesc [18]. Comprehensive evaluation results and ablation studies on two standard descriptor datasets: UBC Phototour [5] (Sec. 5.2), and HPatches [3] (Sec. 5.3) demonstrate the efficacy of our proposed sampling framework.

5.2. UBC Phototour

UBC Phototour [5], also known as Brown dataset, consists of three subsets: *Liberty*, *Notre Dame*, and *Yosemite*, with about 400K normalized 64×64 patches in each subset. Keypoints are detected by DoG detector [17] and verified by 3D model. The testing set consists of 100K matching and non-matching pairs for each sequence. For evaluation, models are trained on one subset and tested on the other two. The metric is the false positive rate (FPR) at 95% true positive recall. The evaluation results are reported in Tab. 1.

Our method outperforms other approaches by a significant margin. We randomly flip and rotate by 90 degrees for

⁵This relation holds only when the hinge triplet loss is positive. Empirically, due to the relatively large margin, the hinge loss never becomes zero.

⁶Note that the training dataset of GeoDesc [18] is not released, so the comparison may be unfair. Besides, some recent works [31, 36] explore in different directions, and their training codes are not publicly available. So we leave the efficacy comparison and system combination in future work.

Descriptor	Length	Train→ Test→	Notredame	Yosemite	Liberty	Yosemite	Liberty	Notredame	Yosemite	Mean
			Liberty		Notredame		Yosemite			
SIFT [17]	128		29.84		22.53		27.29		26.55	
DeepDesc [28]	128		10.9		4.40		5.69		6.99	
GeoDesc [18]	128		5.47		1.94		4.72		4.05	
MatchNet [10]	4096		7.04	11.47	3.82	5.65	11.60	8.70	8.05	
L2-Net [30]	128		3.64	5.29	1.15	1.62	4.43	3.30	3.24	
CS-L2-Net [30]	256		2.55	4.24	0.87	1.39	3.81	2.84	2.61	
HardNet [21]	128		1.47	2.67	0.62	0.88	2.14	1.65	1.57	
HardNet-GOR [37]	128		1.72	2.89	0.63	0.91	2.10	1.59	1.64	
HardNet*	128		1.80	2.89	0.68	0.90	1.93	1.71	1.65	
AdaSample* (Ours)	128		1.64	2.62	0.61	0.88	1.92	1.46	1.52	
TFeat-M+ [4]	128		7.39	10.31	3.06	3.80	8.06	7.24	6.64	
L2-Net+ [30]	128		2.36	4.70	0.72	1.29	2.57	1.71	2.23	
CS-L2-Net+ [30]	256		1.71	3.87	0.56	1.09	2.07	1.30	1.76	
HardNet+ [21]	128		1.49	2.51	0.53	0.78	1.96	1.84	1.51	
HardNet-GOR+ [37]	128		1.48	2.43	0.51	0.78	1.76	1.53	1.41	
DOAP+ [11]	128		1.54	2.62	0.43	0.87	2.00	1.21	1.45	
HardNet+*	128		1.32	2.31	0.41	0.67	1.51	1.24	1.24	
AdaSample+* (Ours)	128		1.25	2.21	0.40	0.63	1.40	1.14	1.17	

Table 1. Patch classification results on UBC Phototour dataset [5]. The false positive rate at 95% recall is reported. + indicates data augmentation and * indicates positive generation.

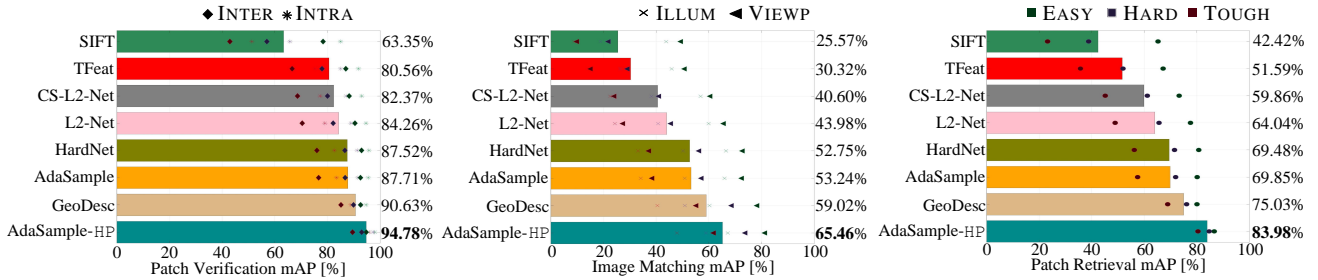


Figure 2. Evaluation results on HPatches dataset [3]. By default, descriptors are trained on *Liberty* subset of UBC Phototour [5] dataset, and “-HP” indicates descriptors trained on HPatches training set of split a. Marker color indicates the level of geometrical noises and marker type indicates the experimental setup. INTER and INTRA indicate the source of negative examples for the *verification* task. VIEWP and ILLUM indicate the sequence type for the *matching* task.

data augmentation, noted by +. Besides, for our method, we also generate positive patches by random rotation such that each class has 15 patches, noted by *. We augment matching pairs as there are too few patches (two or three) corresponding to one class in UBC Phototour dataset [5], which limits the capacity of our method. To analyze its effect, we also conduct it for HardNet [21] baseline. It can be seen that our method consistently outperforms the baseline, indicating the effectiveness of our adaptive sampling solution.

5.3. HPatches

HPatches [3] consists of 116 sequences of 6 images. The dataset is split into two parts: *viewpoint* - 59 sequences with significant viewpoint change and *illumination* - 57 sequences with significant illumination change. According to

the level of geometric noises, the patches can be further divided into three groups: *easy*, *hard*, and *tough*. There are three evaluation tasks: *patch verification*, *image matching*, and *patch retrieval*. Following standard evaluation protocols of the dataset, we show results in Fig. 2. It demonstrates that our method performs in favor of other methods on patch verification task, which is consistent with the patch classification results in Tab. 1. Furthermore, our descriptors achieve the best results on the more challenging image matching and patch retrieval tasks, indicating the improved generalization ability contributed by our approach.

5.4. Ablation Study

Informativeness Approximation. We empirically verify the conclusion in Sec. 4.2 that the probability induced by matching distance approximate well to the one induced by

informativeness (Fig. 3, Left). Besides, the results show that the Pearson correlation is consistently greater than 0.8 during training (Fig. 3, Right), which indicates these probabilities have strong correlation with each other statistically.

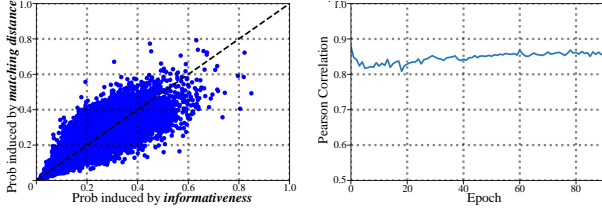


Figure 3. (Left) Probabilities induced by informativeness and matching distance. (Right) Pearson correlation between probabilities and training epochs.

Impact of λ and Distance Metric. We experiment with varying λ in *AdaSample* to control the overall hardness of the selected matching pairs. A large λ indicates that hard matching pairs are more likely to be selected. When $\lambda = 0$, our method degrades into random sampling and the overall framework becomes HardNet [21], and as $\lambda \rightarrow +\infty$, the framework becomes *Hardpos*. Therefore, both HardNet and *Hardpos* are special cases of our proposed *AdaSample*. Tab. 2 shows the results on HPatches [3] dataset, where $\lambda = 10$ leads to the best results in most cases. It demonstrates the advantages of our balanced sampling strategy against the hardest solution. Also, Tab. 2 demonstrates that the angular hinge triplet (AHT) loss outperforms the commonly-used hinge triplet (HT) loss in most cases.

Task	Verification		Matching		Retrieval	
Loss	AHT	HT	AHT	HT	AHT	HT
$\lambda = 1$	93.84	93.17	64.09	62.64	81.26	79.97
$\lambda = 2$	94.72	94.56	66.04	65.92	83.58	83.34
$\lambda = 5$	94.78	94.76	65.89	65.68	83.80	83.54
$\lambda = 10$	94.78	94.60	65.46	65.37	83.98	83.62
$\lambda = 20$	94.60	94.69	64.56	64.84	83.56	83.69
$\lambda \rightarrow +\infty$	94.42	94.51	63.81	64.02	83.41	83.29

Table 2. Ablation studies on the impact of λ . All experiments are conducted on HPatches [3] benchmark.

Stability and Reproducibility. The sampling naturally comes from stochasticity. To ensure reproducibility, we conduct experiments on five runs with different random seeds and show the means and standard deviations of the patch classification results in Tab. 3. It demonstrates the stability of our sampling solution. We argue that a possible explanation of the stability is the *unbiasedness* of the gradient estimator (Eqn. 10). As the number of training triplets is huge, the estimated gradients converge to the actual gradient asymptotically. Therefore, the gradients can guide the network towards the parameter optimum as training progresses, regardless of the specific random condition.

Train	Test	HardNet+*	AdaSample+*	Rel \uparrow	p value
Notr	Lib	1.316 \pm 0.044	1.254 \pm 0.026	4.71%	0.031
Yos		2.310 \pm 0.063	2.212 \pm 0.049	4.28%	0.018
Lib	Notr	0.406 \pm 0.011	0.400 \pm 0.016	1.58%	0.337
Yos		0.671 \pm 0.010	0.627 \pm 0.012	6.62%	0.006
Lib	Yos	1.513 \pm 0.084	1.395 \pm 0.050	7.80%	0.030
Notr		1.241 \pm 0.044	1.137 \pm 0.036	8.38%	0.011

Table 3. Reproducibility and statistical significance of our proposed *AdaSample*. The repeated experiments are conducted on UBC Phototour [5] dataset. Here, “Rel \uparrow ” indicates the relative improvement upon the HardNet [21] baseline.

Statistical Significance. Since previous methods have been approaching the saturating point in terms of the performance on UBC Phototour [5] dataset, it is challenging to make progress on top of the HardNet [21] baseline. However, with the proposed method, we still observe a consistent improvement, as demonstrated in Tab. 3. It can be seen that our method can give a relative improvement of up to 8.38% in terms of patch classification accuracy, indicating our superiority. To be more principled, we also demonstrate the statistical significance of our improvement upon the baseline. Specifically, we adopt the non-parametric hypothesis testing, *i.e.*, the classic Mann-Whitney testing [19], to test whether a random variable is stochastically larger than the other one. In our setting, the two random variables are the performance of *AdaSample* and HardNet baseline, respectively, and the null hypothesis is that our method *cannot* significantly improve the performance. The p values under different experimental settings are summarized in Tab. 3. With a significance level of $\alpha = 5\%$, we can reject the null hypothesis in 5 of the 6 experiments in total. For the only anomaly, *i.e.*, training on Notre Dame and testing on Liberty, we conjecture that the reason lies in the extremely high performance of the HardNet baseline (about 0.4% in terms of FPR). Therefore, we argue that the statistical significance under the other 5 experimental settings is sufficient to verify the effectiveness of our approach.

6. Conclusion

This paper proposes *AdaSample* for descriptor learning, which adaptively samples hard positives to construct informative mini-batches during training. We demonstrate the efficacy of our method from both theoretical and empirical perspectives. Theoretically, we give a rigorous definition of *informativeness* of potential training examples. Then, we reformulate the problem and derive a tractable sampling probability expression (Eqn. 13) to generate hardness-aware training triplets. Empirically, we enjoy a consistent and statistically significant performance gain on top of the HardNet [21] baseline when evaluated on various tasks, including patch classification, patch verification, image matching, and patch retrieval.

References

- [1] Sameer Agarwal, Noah Snavely, Ian Simon, Steven M Seitz, and Richard Szeliski. Building rome in a day. In *IEEE International Conference on Computer Vision (ICCV)*, pages 72–79. IEEE, 2009.
- [2] Jimmy Lei Ba, Jamie Ryan Kiros, and Geoffrey E Hinton. Layer normalization. *arXiv preprint arXiv:1607.06450*, 2016.
- [3] Vassileios Balntas, Karel Lenc, Andrea Vedaldi, and Krystian Mikolajczyk. HPatches: A benchmark and evaluation of handcrafted and learned local descriptors. In *IEEE Conference on Computer Vision and Pattern Recognition (CVPR)*, pages 5173–5182, 2017.
- [4] Vassileios Balntas, Edgar Riba, Daniel Ponsa, and Krystian Mikolajczyk. Learning local feature descriptors with triplets and shallow convolutional neural networks. In *British Machine Vision Conference (BMVC)*, 2016.
- [5] Matthew Brown, Gang Hua, and Simon Winder. Discriminative learning of local image descriptors. *IEEE Transactions on Pattern Recognition and Machine Intelligence (PAMI)*, 33(1):43–57, 2011.
- [6] Matthew Brown and David G Lowe. Automatic panoramic image stitching using invariant features. *International Journal on Computer Vision (IJCV)*, 74(1):59–73, 2007.
- [7] Jiankang Deng, Jia Guo, Niannan Xue, and Stefanos Zafeiriou. ArcFace: Additive angular margin loss for deep face recognition. In *IEEE Conference on Computer Vision and Pattern Recognition (CVPR)*, pages 4690–4699, 2019.
- [8] Jack Edmonds. Matroids and the greedy algorithm. *Mathematical programming*, 1(1):127–136, 1971.
- [9] Xavier Glorot and Yoshua Bengio. Understanding the difficulty of training deep feedforward neural networks. In *Proceedings of the thirteenth international conference on artificial intelligence and statistics*, pages 249–256, 2010.
- [10] Xufeng Han, Thomas Leung, Yangqing Jia, Rahul Sukthankar, and Alexander C Berg. Matchnet: Unifying feature and metric learning for patch-based matching. In *IEEE Conference on Computer Vision and Pattern Recognition (CVPR)*, pages 3279–3286, 2015.
- [11] Kun He, Yan Lu, and Stan Sclaroff. Local descriptors optimized for average precision. In *IEEE Conference on Computer Vision and Pattern Recognition (CVPR)*, pages 596–605, 2018.
- [12] Kaiming He, Xiangyu Zhang, Shaoqing Ren, and Jian Sun. Delving deep into rectifiers: Surpassing human-level performance on imagenet classification. In *IEEE International Conference on Computer Vision (ICCV)*, pages 1026–1034, 2015.
- [13] Sergey Ioffe and Christian Szegedy. Batch Normalization: Accelerating deep network training by reducing internal covariate shift. In *International Conference on Machine Learning (ICML)*, pages 448–456, 2015.
- [14] Angelos Katharopoulos and François Fleuret. Not all samples are created equal: Deep learning with importance sampling. *PMLR*, pages 2525–2534, 2018.
- [15] Yan Ke, Rahul Sukthankar, et al. PCA-SIFT: A more distinctive representation for local image descriptors. In *IEEE Conference on Computer Vision and Pattern Recognition (CVPR)*, pages 506–513, 2004.
- [16] Tsung-Yi Lin, Priya Goyal, Ross Girshick, Kaiming He, and Piotr Dollár. Focal loss for dense object detection. In *IEEE International Conference on Computer Vision (ICCV)*, pages 2980–2988, 2017.
- [17] David G Lowe. Distinctive image features from scale-invariant keypoints. *International Journal on Computer Vision (IJCV)*, 60(2):91–110, 2004.
- [18] Zixin Luo, Tianwei Shen, Lei Zhou, Siyu Zhu, Runze Zhang, Yao Yao, Tian Fang, and Long Quan. GeoDesc: Learning local descriptors by integrating geometry constraints. In *European Conference on Computer Vision (ECCV)*, pages 168–183, 2018.
- [19] Henry B Mann and Donald R Whitney. On a test of whether one of two random variables is stochastically larger than the other. *The annals of mathematical statistics*, pages 50–60, 1947.
- [20] Krystian Mikolajczyk and Cordelia Schmid. A performance evaluation of local descriptors. *IEEE Transactions on Pattern Recognition and Machine Intelligence (PAMI)*, pages 1615–1630, 2005.
- [21] Anastasiia Mishchuk, Dmytro Mishkin, Filip Radenovic, and Jiri Matas. Working hard to know your neighbor’s margins: Local descriptor learning loss. In *Neural Information Processing Systems (NIPS)*, pages 4826–4837, 2017.
- [22] Eric Moulines and Francis R Bach. Non-asymptotic analysis of stochastic approximation algorithms for machine learning. In *Neural Information Processing Systems (NIPS)*, pages 451–459, 2011.
- [23] Deanna Needell, Rachel Ward, and Nati Srebro. Stochastic gradient descent, weighted sampling, and the randomized kaczmarz algorithm. In *Neural Information Processing Systems (NIPS)*, pages 1017–1025, 2014.
- [24] James Philbin, Michael Isard, Josef Sivic, and Andrew Zisserman. Descriptor learning for efficient retrieval. In *European Conference on Computer Vision (ECCV)*, pages 677–691. Springer, 2010.
- [25] Florian Schroff, Dmitry Kalenichenko, and James Philbin. FaceNet: A unified embedding for face recognition and clustering. In *IEEE Conference on Computer Vision and Pattern Recognition (CVPR)*, pages 815–823, 2015.
- [26] Shai Shalev-Shwartz and Yonatan Wexler. Minimizing the maximal loss: How and why. In *International Conference on Machine Learning (ICML)*, pages 793–801, 2016.
- [27] Edgar Simo-Serra, Eduard Trulls, Luis Ferraz, Iasonas Kokkinos, Pascal Fua, and Francesc Moreno-Noguer. Discriminative learning of deep convolutional feature point descriptors. In *IEEE International Conference on Computer Vision (ICCV)*, pages 118–126, 2015.
- [28] E. Simo-Serra, E. Trulls, L. Ferraz, I. Kokkinos, P. Fua, and F. Moreno-Noguer. Discriminative learning of deep convolutional feature point descriptors. In *IEEE International Conference on Computer Vision (ICCV)*, pages 118–126, Dec 2015.
- [29] Benoit Steiner, Zachary DeVito, Soumith Chintala, Sam Gross, Adam Paszke, Francisco Massa, Adam Lerer, Gregory Chanan, Zeming Lin, Edward Yang, et al. Pytorch: An

- imperative style, high-performance deep learning library. In *Neural Information Processing Systems (NIPS)*, 2019.
- [30] Yurun Tian, Bin Fan, and Fuchao Wu. L2-Net: Deep learning of discriminative patch descriptor in euclidean space. In *IEEE Conference on Computer Vision and Pattern Recognition (CVPR)*, pages 661–669, 2017.
 - [31] Yurun Tian, Xin Yu, Bin Fan, Fuchao Wu, Huub Heijnen, and Vassileios Balntas. SOSNet: Second order similarity regularization for local descriptor learning. In *IEEE Conference on Computer Vision and Pattern Recognition (CVPR)*, 2019.
 - [32] Dmitry Ulyanov, Andrea Vedaldi, and Victor Lempitsky. Instance Normalization: The missing ingredient for fast stylization. *arXiv preprint arXiv:1607.08022*, 2016.
 - [33] Chao-Yuan Wu, R Manmatha, Alexander J Smola, and Philipp Krahenbuhl. Sampling matters in deep embedding learning. In *IEEE International Conference on Computer Vision (ICCV)*, pages 2840–2848, 2017.
 - [34] Kwang Moo Yi, Eduard Trulls, Vincent Lepetit, and Pascal Fua. LIFT: Learned invariant feature transform. In *European Conference on Computer Vision (ECCV)*, pages 467–483. Springer, 2016.
 - [35] Sergey Zagoruyko and Nikos Komodakis. Learning to compare image patches via convolutional neural networks. In *IEEE Conference on Computer Vision and Pattern Recognition (CVPR)*, pages 4353–4361, 2015.
 - [36] Linguang Zhang and Szymon Rusinkiewicz. Learning local descriptors with a cdf-based dynamic soft margin. In *IEEE Conference on Computer Vision and Pattern Recognition (CVPR)*, pages 2969–2978, 2019.
 - [37] Xu Zhang, Felix X Yu, Sanjiv Kumar, and Shih-Fu Chang. Learning spread-out local feature descriptors. In *IEEE Conference on Computer Vision and Pattern Recognition (CVPR)*, pages 4595–4603, 2017.
 - [38] Wenzhao Zheng, Zhaodong Chen, Jiwen Lu, and Jie Zhou. Hardness-Aware deep metric learning. In *IEEE Conference on Computer Vision and Pattern Recognition (CVPR)*, pages 72–81, 2019.